Stansell et al. GSA DATA REPOSITORY

Age-Depth model

The age-depth model for the El Gancho sediment record is based on radiocarbon ages of charcoal samples picked using metal tweezers under a binocular microscope (Fig. DR1 and Table DR1). Samples were pre-treated using standard acid-base-acid protocols (Abbott and Stafford, 1996). Analyses were conducted at the W.M. Keck Carbon Cycle Accelerator Mass Spectrometry Laboratory at the University of California, Irvine (UCI). Radiocarbon ages were converted to calendar ages using OxCal 4.2, and the Intcal 09 dataset (Reimer et al., 2009). Sediment age and depth were related using a 3rd order polynomial fit (R^2=0.99) between the median calibrated ages. The details of the modeled age-depth values are presented in Figure DR1, and a simplified version is presented in Figure 2 of the main text.

No suitable organic material for radiocarbon dating was found in the lower ~40 cm of the El Gancho sediment core. The basal sediments are not typical lacustrine deposits, and are the result of a dry debris avalanche on the northeast flank of Vólcan Mombacho (van Wyk de Vries and Francis, 1997; Shea et al., 2008). Therefore, the age-depth model was not applied to the lower ~40 cm of the record.

Fieldwork

The water depth of El Gancho was surveyed using a handheld sonar system in June, 2004. A 277 cm-long composite core with overlapping sections was retrieved from the depocenter of the lake (1.1 m) using a Livingstone piston corer and extruded in the field into split PVC tubes. Surface sediments were collected using a polycarbonate tube attached to a percussion corer, and the upper 34 cm of flocculent material was extruded in the field at 0.5 cm intervals into plastic bags. Water samples from 11 sites in Nicaragua were collected during May,

2003 and June, 2004 in 30 mL high-density polyethylene bottles for oxygen and hydrogen isotope analyses (Fig. 3 and Table DR2).

Modern Water Chemistry

Hydrogen (δD) and oxygen isotopic ratios of surface water samples were measured at the University of Arizona Environmental Isotope Laboratory by CO_2 equilibration with a VG602C Finnigan® Delta S isotope ratio mass spectrometer (Table DR2). All values are expressed in standard per mil (‰) notation on the Vienna Standard Mean Ocean Water (VSMOW) scale. The reported precision is 0.1 ‰ for $\delta^{18}O$ and 1.0 ‰ for δD. Water isotope data were plotted relative to the global meteoric water line (GMWL) to demonstrate the extent of evaporative enrichment within El Gancho surface water (Fig. 3).

Stable isotope and Sedimentological measurements

Sediment samples for isotope analyses were disaggregated with 7 % H_2O_2 and sieved using a 63 μm screen. The >63 μm sediment fraction was dried on filter paper at 60° C for 12 hours and dry sieved at 150 μm to isolate macrofossil remains. Ostracod valves were soaked in 15 % H_2O_2, cleaned ultrasonically in deionized water, rinsed with methanol and dried at 60°C for 12 hours. Aggregates of ~30 ostracod carapaces from each sample were reacted in 100 % phosphoric acid at 90ºC, and measured at the University of Pittsburgh using a dual-inlet GV Instruments, Ltd. IsoPrime™ stable isotope ratio mass spectrometer equipped with a dual inlet, MultiPrep™ module and Gilson autosampler. The analytical precision is 0.1‰ for oxygen. Samples were measured against National Institute of Standards and Technology (NIST) carbonate standard material NBS-18 and NBS-19 and reported relative to the VPDB isotope scale in standard delta (δ) and per mil (‰) notation.

Organic matter and carbonate content were measured on 1 cm^3 samples at 2 to 5 cm resolution by loss-on-ignition (LOI) at 550°C and 1000°C, respectively (Dean Jr., 1974; Heiri et al., 2001; Boyle, 2004) (Fig. DR2). Volume magnetic susceptibility (MS) was measured on split cores every 0.5 cm using a Bartington high-resolution surface-scanning sensor connected to a susceptibility meter. The residual (%) LOI values of the El Gancho sediments (Fig. DR2) generally track changes in magnetic susceptibility (MS). For example, the highest measured MS values of the record are found in the basal section of the core (below A.D. 300), which is characterized by low organic matter and calcium carbonate concentrations, and high LOI residual values. Above a depth corresponding to A.D. 300, LOI residual and magnetic susceptibility values markedly decrease, suggesting that sedimentation in the lake basin stabilized at this time.

Lake modeling

Hydrologic and isotope mass balance models have been used to investigate lake sensitivity to specific climate variables (Gibson et al., 2002; Shapley et al., 2008; Jones and Imbers, 2010) and to develop a basis for the paleo-interpretation of sediment geochemical records (Rowe and Dunbar, 2004; Jones et al., 2007; Roberts et al., 2008). Here we apply a simple lake hydrologic and isotope mass balance model (based on the work of Steinman et al. 2010a; 2010b) to characterize the isotopic responses of El Gancho water and sediment biogenic calcite to changes in precipitation, temperature, and relative humidity. These hydroclimatic variables, as well as catchment parameters and basin morphology, control water balance and lake residence time and therefore determine lake geochemical responses to climate dynamics on time scales ranging from months to millennia. We use the model simulations presented herein as a framework for the interpretation of the El Gancho $\delta^{18}O_{ostracod}$ record.

Model structure

The hydrologic and isotope mass balance model applied here is based on the lake-catchment model of Steinman et al. (2010a) (Table DR4). To adapt this model to El Gancho, we removed the catchment components and developed a simplified lake water input algorithm that simulates groundwater flow and catchment runoff into the lake. Such approximations were necessary given the lack of information on El Gancho lake catchment hydrologic characteristics. Consequently, the model presented here is meant for simulating the general isotope dynamics of a shallow, seasonally overflowing lake with a large surface area to volume ratio located in a tropical climatic setting with a seasonal distribution of precipitation (i.e., a lake that is similar but not necessarily identical to El Gancho).

The model presented here is defined by a system of four ordinary differential equations compiled using STELLA® (isee systems ™) software. The model equations integrate a system of two water reservoirs (notated as *RES* in the equations that follow) and volumetric fluxes (*F*) to the reservoirs. A series of steady state simulations were conducted to investigate long-term (i.e., multidecadal) lake responses to climate forcing. Simulations were conducted on a monthly time step (with eight iterations calculated for each month) using average monthly climate data (Table DR3).

Hydrologic mass-balance equations

The model calculates mass balance through time for the lake reservoir (RES_L) by the volumetric addition of direct precipitation over the lake area (F_P) and inflow (F_{IN}) from the catchment/groundwater reservoir (RES_{CG}), and subtraction of lake water evaporation (F_E) and overflow (F_{OUT}). Mass balance for the catchment/groundwater inflow reservoir (RES_{CG}) is determined by the addition of a parameterized precipitation input flux (F_{CP}) and the subtraction

of water flowing into the lake (F_{IN}). RES_{CG} is not meant to represent a reservoir in nature but rather is an empirical construct designed to approximate groundwater and catchment water flowing into the lake. Outseepage from the lake is assumed to be negligible (relative to overflow) and therefore is not included as a separate flux variable.

Lake water mass-balance is described by the following equations, utilizing the notation above:

$$\frac{dRES_L}{dt} = F_P + F_{IN} - F_E - F_{OUT} \tag{1}$$

$$\frac{dRES_{CG}}{dt} = F_{CP} - F_{IN} \tag{2}$$

where direct precipitation over the lake (F_P) is determined by multiplying monthly precipitation amounts (see ***Model inputs***, below; Table DR3) by the lake surface area (SA). Evaporation from the lake surface (F_E) is estimated using a combined radiation-aerodynamic Penman equation and is calculated by multiplying monthly evaporation by the lake surface area.

Overflow (F_{OUT}) is calculated in accordance with the following equation:

$$F_{OUT} = \begin{cases} \left(RES_L - 35750\ \mathrm{m}^3\right) \times dt^{-1} & RES_L > 35750\ \mathrm{m}^3 \\ 0 & RES_L \leq 35750\ \mathrm{m}^3 \end{cases} \tag{3}$$

where 35750 m^3 represents the overflow volume based on field observations of overflow occurring at a depth of ~1.1 m and a lake surface area of 32500 m^2 (estimated using satellite imagery).

The flux of inflowing water derived from catchment and groundwater (F_{IN}) as well as the flux of water flowing into the catchment groundwater reservoir (RES_{CG}) are determined by:

$$F_{IN} = RES_{CG} \times C_{IN} \times dt^{-1} \tag{4}$$

$$F_{CP} = P \times C_{CP} \times dt^{-1} \tag{5}$$

where constants, C_{IN} and C_{CP}, are derived through a simple calibration process (see ***Model Calibration***, below) and P is monthly precipitation in meters.

Lake evaporation model sub-routine

The evaporation model is a simplified version of the modified Penman equation (Valiantzas, 2006) and was chosen on the basis of available meteorological data and the fact that it produces values that are similar to those of the energy budget method for calculating evaporation (Rosenberry et al., 2007).

Isotope mass-balance equations

The reservoir and flux structure of the isotope mass-balance model is identical to that of the hydrologic model and follows the equations of Dinçer (1968), Gonfiantini (1986), and Gat (1995). Oxygen and hydrogen isotope values, in standard delta (δ) notation as the per mil (‰) deviation from Vienna Standard Mean Ocean Water (VSMOW), are calculated for each reservoir at each time step and are multiplied by the corresponding hydrologic flux to determine the isotope mass-balance of any given water mass.

The linear resistance model of Craig and Gordon (1965) is used to calculate the isotopic composition of water evaporating from the lake surface (δ_E):

$$\delta_E = \frac{\alpha^* \delta_L - h_n \delta_A - \varepsilon_{tot}}{1 - h_n + 0.001\varepsilon_k} \tag{6}$$

where α^* is the reciprocal of the equilibrium isotopic fractionation factor, δ_L is the isotopic composition of lake water, h_n is the ambient humidity normalized to lake water temperature, δ_A, is the isotopic composition of atmospheric moisture, ε_{tot} is the total per mil isotopic separation ($\varepsilon_{eq} + \varepsilon_k$), ε_{eq} is the equilibrium isotopic separation, and ε_k is the kinetic isotopic separation.

The saturation vapor pressure of the overlying air ($e_{s\text{-}a}$) and the saturation vapor pressure at the surface water temperature ($e_{s\text{-}w}$) in millibars are used to determine the normalized relative

humidity (h_n). Atmospheric moisture (δ_A) is assumed to be at isotopic equilibrium with precipitation (Gibson et al., 2002). The equilibrium isotopic fractionation factor (α) and the reciprocal of the equilibrium isotopic fractionation factor (α^*) for oxygen and hydrogen are calculated using the equations of (Horita and Wesolowski, 1994). Kinetic fractionation (ε_k) is controlled by molecular diffusion and the moisture deficit ($1 - h_n$) over the lake surface (Merlivat and Jouzel, 1979), wherein the experimentally derived isotopic separation values (C) of 14.3 ‰ for oxygen and 12.4 ‰ for hydrogen are applied (Vogt, 1976; Araguas et al., 2000). Subroutines that calculate sediment $\delta^{18}O$ values on the VPDB (Vienna Pee Dee Belemnite) scale were also added to the model, in order to simulate the isotopic composition of ostracod calcite. The model calculates the equilibrium fractionation factor for ostracod bio-calcite using the equation of Kim and O'Neil (1997). Values for $\alpha_{calcite}$ are related to lake water $\delta^{18}O$ values on the VSMOW (Vienna Standard Mean Ocean Water) scale in accordance with the standard isotope fractionation relationship:

$$\alpha_{calcite} = \frac{1000 + \delta_C}{1000 + \delta_L} \tag{7}$$

where $\alpha_{calcite}$ is the fractionation factor of the calcite-water system, δ_C is the isotopic composition of calcite, and δ_L is the isotopic composition of lake water. The model converts theoretical calcite $\delta^{18}O$ values from the VSMOW to the VPDB scale using the following standard equation:

$$\delta_{VSMOW} = 1.03092 \times \delta_{VPDB} + 30.92 \tag{8}$$

The model also applies an isotopic offset of +1 ‰ to bio-calcite $\delta^{18}O$ values to simulate the vital isotopic effect associated with ostracod carapace production. Note that this vital offset value is an estimate based on measured values for other non-Candonid ostracods (von Grafenstein et al., 1999).

Model inputs

Steady state and continuous model simulations utilized monthly weather data derived from satellite and weather station measurements (Table DR3). Specifically, average monthly precipitation (P) and incoming solar insolation (R_s) were defined using ~30 years of continuous weather station data from Managua (Portig, 1976). Extraterrestrial solar insolation (R_a) was based on estimates obtained from the NASA Monthly Latitude Insolation website (http://aom.giss.nasa.gov/srmonlat.html). Monthly average values for relative humidity (RH) and air temperature (T_a) were based on the satellite derived estimates of (1000 hPa pressure level) (Rienecker et al., 2011). Average wind speed (WS) and average lake water temperature (T_w) are unknown and were estimated to be ~2 m/s and +2.5 °C relative to air temperature, respectively. Monthly $\delta^{18}O$ and δD values of precipitation were estimated using the interpolated values of Bowen and Revenaugh (2003) (waterisotopes.org). Lake surface area was estimated using satellite imagery and topographic maps. Because El Gancho is at or near overflow at all times, the model maintains a constant lake surface area throughout all simulations.

Model simulations

All model simulations were conducted with the STELLA® software using the fourth order Runge-Kutta numerical integration method. In the first series of model simulations (***Model calibration***), monthly average climate data were used to estimate lake model constants (C_{CG} and C_{IN}, above) and to thereby balance the model at lake depths and $\delta^{18}O$ values consistent with observations. Lake water δD values were also simulated in order to compare modeled and observed regional evaporation lines as a validation test for the isotopic components of the model. The second series of simulations (***Model sensitivity to climate variables***) were designed to evaluate the sensitivity of El Gancho to each of the primary hydroclimatic variables (i.e.,

precipitation, relative humidity, and temperature).

Model calibration

The catchment precipitation constant (C_{CP}) determines the flux of water (as a function of P) into the catchment/groundwater reservoir (RES_{CG}). Steady state simulations were conducted in which C_{CP} was adjusted downward from a value of 100 to a value of 50, at which point modeled lake depth and $\delta^{18}O$ values were similar to observations. After balancing the model at steady state, C_{IN} was assigned a value of 0.1, which reduced F_{IN} values to 10 % of RES_{CG}, in order to approximate precipitation transit times through the catchment via surface and groundwater pathways. In this configuration model simulations produced a realistic pattern of seasonal lake water and ostracod $\delta^{18}O$ variations, with minimum values in November and maximum values in May, as well as average annual ostracod $\delta^{18}O$ values that are similar to measured values in the El Gancho sediment core (Fig. DR3).

Steady state model simulations with identical climate forcing were then conducted using hydrogen isotope mass balance components. These data were combined with $\delta^{18}O$ data to produce a model derived regional evaporation line (REL) (Fig. 3), which was used to validate model isotopic subroutines as well as parameter values obtained through the calibration exercise. Modeled lake surface water δD values were similar to measured δD values, and produced a theoretical relative evaporation line with a slope (~5.0) very similar to that derived from lake surface water measurements. The ability of the model to simulate hydrogen isotope variability demonstrates that the structure of the hydrologic and isotopic model is a reasonable approximation of the El Gancho lake/climate system.

Model sensitivity to climate variables

The objective of the second series of simulations was to determine the long-term

hydrologic and isotopic sensitivity of El Gancho to temperature, relative humidity, and precipitation changes. Tests were also conducted to determine model sensitivity to the catchment hydrologic parameters identified above. In each set of sensitivity tests, simulations were conducted on a monthly time-step over 1000 model months (~83 years) using modern catchment parameters and average, monthly instrumental climate data. In the 501st month, the tested climate variable was either increased or decreased by a constant amount and maintained until the end of the test.

Temperature sensitivity tests

Changes in atmospheric temperature can influence lake hydrologic and isotopic balance by altering evaporative flux from the lake surface, catchment evapotranspiration rates, normalized *RH* values, and the liquid-vapor equilibrium fractionation factor for evaporating water. Atmospheric temperature changes of ±2 °C resulted in average annual water and ostracod $\delta^{18}O$ offsets of less than 0.1 and 0.4 ‰, respectively (Table DR5), suggesting that lake isotope dynamics are relatively insensitive to temperature changes.

Relative Humidity sensitivity tests

The sensitivity of lakes to changes in relative humidity is due to the effect of *RH* on the kinetic fractionation process that occurs during evaporation from the lake surface as well as the influence of RH on evaporation rates. The isotopic responses of El Gancho water and ostracods to *RH* changes of ±5 % was ~0.7 ‰ in both forcing scenarios (Table DR3).

Precipitation sensitivity tests

In response to a precipitation changes of ±50 %, El Gancho exhibited water and ostracod $\delta^{18}O$ increases of >1.5 ‰ and decreases of >1.0 ‰, respectively, largely as a result of hydrologic control on the lake water residence time (Table DR3). For example, larger precipitation amounts

produced greater catchment water influx to the lake, greater wet season overflow rates, and a consequent reduction in water residence time, and vice versa.

Calibration sensitivity tests

Changes in the catchment precipitation constant (C_{CP}) of ±50 % (which corresponds to values of ±25) resulted in $\delta^{18}O$ value differences of ~1.7 ‰ (Table DR5; Fig. DR4). In contrast, adjustments to the catchment inflow delay constant (C_{IN}) of ±50 % (i.e., ±0.5) did not significantly affect average annual water and ostracod $\delta^{18}O$ values. The large sensitivity of the El Gancho model to the catchment precipitation parameter is not unexpected, given the strong control of lake hydrologic balance on water oxygen isotope content. This strong isotopic sensitivity to water influx rates is also demonstrated by the precipitation sensitivity tests.

El Gancho climate sensitivity

The simulation results presented here demonstrate that El Gancho water (and ostracod) $\delta^{18}O$ values are highly sensitive to precipitation amounts and the resulting influence on lake hydrology. Relative humidity also exerts a strong influence on water and sediment $\delta^{18}O$ values through control of the kinetic isotopic separation and the oxygen isotope content of evaporating water. Given that higher *RH* values are likely to occur when conditions are wetter (i.e., precipitation amounts are greater) it is likely that a significant amount of variability in the El Gancho $\delta^{18}O$ record can be explained by *RH* changes. Temperature appears to be a lesser control due to the offsetting hydrologic and isotopic effects of temperature changes on water and calcite $\delta^{18}O$ values. When temperatures increase, for example, the calcite-water fractionation factor decreases, leading to an isotopic depletion of ostracod calcite that is larger in magnitude than the isotopic enrichment resulting from higher evaporation rates and reduced catchment water influx to the lake.

REFERENCES CITED

Abbott, M.B., and Stafford, T.W., 1996, Radiocarbon Geochemistry of Modern and Ancient Arctic Lake Systems, Baffin Island, Canada: Quaternary Research, v. 45, p. 300-311.

Araguas, L.A., Froelich, K., and Rozanski, K., 2000, Deuterium and oxygen-18 isotope composition of precipitation and atmospheric moisture: Hydrological Processes, v. 14, p. 1341-1355.

Bowen, G.J., and Revenaugh, J., 2003, Interpolating the isotopic composition of modern meteoric precipitation: Water Resour. Res., v. 39, p. 1299.

Boyle, J., 2004, A comparison of two methods for estimating the organic matter content of sediments: Journal of Paleolimnology, v. 31, p. 125-127.

Bronk Ramsey, C., 2008, Deposition models for chronological records: Quaternary Science Reviews, v. 27, p. 42-60.

Craig, H., and Gordon, L.I., 1965, Deuterium and oxygen-18 variations in the ocean and the marine atmosphere, *in* Tongiorgi, E., ed., Stable Isotopes in Oceanographic Studies and Paleotemperatures: Pisa, Consiglio Nazionale delle Richerche, Laboratorio di Geologica.

Dean Jr., W.E., 1974, Determination of carbonate and organic matter in calcareous sediments and sedimentary rocks by loss on ignition: comparison with other methods: Journal of Sedimentary Petrology, v. 44, p. 242-248.

Dinçer, T., 1968, The use of oxygen-18 and deuterium concentrations in the water balance of lakes, v. 4, p. 1289-1306.

Gat, J.R., 1995, Stable Isotopes of Fresh and Saline Lakes, *in* Lerman, A., Imboden, D.M., and Gat, J.R., eds., The Physics and Chemistry of Lakes: New York, Springer-Verlag, p. 139-164.

Gibson, J.J., Prepas, E.E., and McEachern, P., 2002, Quantitative comparison of lake throughflow, residency, and catchment runoff using stable isotopes: modelling and results from a regional survey of Boreal lakes: Journal of Hydrology, v. 262, p. 128-144.

Gonfiantini, R., 1986, Environmental Isotopes in Lake Studies, *in* Fritz, P., and Fontes, J.C., eds., Handbook of Environmental Isotope Geochemistry, Volume 2: New York, Elsevier, p. 112-168.

Heiri, O., Lotter, A.F., and Lemcke, G., 2001, Loss on ignition as a method for estimating organic and carbonate content in sediments: reproducibility and comparability of results: Journal of Paleolimnology, v. 25, p. 101-110.

Horita, J., and Wesolowski, D.J., 1994, Liquid-vapor fractionation of oxygen and hydrogen isotopes of water from the freezing to the critical temperature: Geochimica et Cosmochimica Acta, v. 58, p. 3425-3437.

Jones, M.D., and Imbers, J., 2010, Modeling Mediterranean lake isotope variability: Global and Planetary Change, v. 71, p. 193-200.

Jones, M.D., Roberts, C.N., and Leng, M.J., 2007, Quantifying climatic change through the last glacialâ€“interglacial transition based on lake isotope palaeohydrology from central Turkey: Quaternary Research, v. 67, p. 463-473.

Kim, S.-T., and O'Neil, J.R., 1997, Equilibrium and nonequilibrium oxygen isotope effects in synthetic carbonates: Geochimica et Cosmochimica Acta, v. 61, p. 3461-3475.

Lawrimore, J.H., Menne, M.J., Gleason, B.E., Williams, C.N., Wuertz, D.B., Vose, R.S., and Rennie, J., 2011, An overview of the Global Historical Climatology Network monthly mean temperature data set, version 3: J. Geophys. Res., v. 116, p. D19121.

Merlivat, L., and Jouzel, J., 1979, Global Climatic Interpretation of the Deuterium-Oxygen-18 Relationship for Precipitation: Journal of Geophysical Research, v. 84, p. 5029-5033.
Portig, W.H., 1976, The climate of Central America, *in* Schwerdtfeger, W., ed., World Survey of Climatology, Volume 12: Madison, Elsevier Scientific Publishing Company.
Reimer, P.J., Baillie, M.G.L., Bard, E., Bayliss, A., Beck, J.W., Blackwell, P.G., Bronk Ramsey, C., Buck, C.E., Burr, G.S., Edwards, R.L., Friedrich, M., Grootes, P.M., Guilderson, T.P., Hajdas, I., Heaton, T.J., Hogg, A.G., Hughen, K.A., Kaiser, K.F., Kromer, B., McCormac, G., Reimer, R.W., Richards, D.A., Southon, J.R., Talamo, S., Turney, C.S.M., van der Plicht, J., and Weyhenmeyer, C., 2009, IntCal09 and Marine09 radiocarbon age calibration curves, 0-50,000 years cal BP: Radiocarbon, v. 51, p. 1111-1150.
Rienecker, M.M., Suarez, M.J., Gelaro, R., Todling, R., Bacmeister, J., Liu, E., Bosilovich, M.G., Schubert, S.D., Takacs, L., Kim, G.-K., Bloom, S., Chen, J., Collins, D., Conaty, A., da Silva, A., Gu, W., Joiner, J., Koster, R.D., Lucchesi, R., Molod, A., Owens, T., Pawson, S., Pegion, P., Redder, C.R., Reichle, R., Robertson, F.R., Ruddick, A.G., Sienkiewicz, M., and Woollen, J., 2011, MERRA: NASA's Modern-Era Retrospective Analysis for Research and Applications: Journal of Climate, v. 24, p. 3624-3648.
Roberts, N., Jones, M.D., Benkaddour, A., Eastwood, W.J., Filippi, M.L., Frogley, M.R., Lamb, H.F., Leng, M.J., Reed, J.M., Stein, M., Stevens, L., Valero-GarcÃ©s, B., and Zanchetta, G., 2008, Stable isotope records of Late Quaternary climate and hydrology from Mediterranean lakes: the ISOMED synthesis: Quaternary Science Reviews, v. 27, p. 2426-2441.
Rosenberry, D.O., Winter, T.C., Buso, D.C., and Likens, G.E., 2007, Comparison of 15 evaporation methods applied to a small mountain lake in the northeastern USA: Journal of Hydrology, v. 340, p. 149-166.
Rowe, H.D., and Dunbar, R.B., 2004, Hydrologic-energy balance constraints on the Holocene lake-level history of lake Titicaca, South America: Climate Dynamics, v. 23, p. 439-454.
Shapley, M., Ito, E., and Donovan, J., 2008, Isotopic evolution and climate paleorecords: modeling boundary effects in groundwater-dominated lakes: Journal of Paleolimnology, v. 39, p. 17-33.
Shea, T., van Wyk de Vries, B., and Pilato, M., 2008, Emplacement mechanisms of contrasting debris avalanches at Volcán Mombacho (Nicaragua), provided by structural and facies analysis: Bulletin of Volcanology, v. 70, p. 899.
Steinman, B.A., Rosenmeier, M.F., and Abbott, M.B., 2010a, The isotopic and hydrologic response of small, closed-basin lakes to climate forcing from predictive models: simulations of stochastic and mean-state precipitation variations: Limnology and Oceanography, v. 55, p. 2246-2261.
Steinman, B.A., Rosenmeier, M.F., Abbott, M.B., and Bain, D.J., 2010b, The isotopic and hydrologic response of small, closed-basin lakes to climate forcing from predictive models: application to paleoclimate studies in the upper Columbia River basin: Limnology and Oceanography, v. 55, p. 2231-2245.
Valiantzas, J.D., 2006, Simplified versions for the Penman evaporation equation using routine weather data: Journal of Hydrology, v. 331, p. 690-702.
van Wyk de Vries, B., and Francis, P.W., 1997, Catastrophic collapse at stratovolcanoes induced by gradual volcano spreading: Nature, v. 387, p. 387-390.

Vogt, H.J., 1976, Separation of isotopes in the evaporation of water: Staatsexamensarbeit, Universitat Heidelberg.
von Grafenstein, U., Erlernkeuser, H., and Trimborn, P., 1999, Oxygen and carbon isotopes in modern fresh-water ostracod valves: assessing vital offsets and autecological effects of interest for palaeoclimate studies: Palaeogeography, Palaeoclimatology, Palaeoecology, v. 148, p. 133.

Table DR1. Measured and calibrated radiocarbon ages for charcoal samples from El Gancho. The calibrated age ranges were calculated using OxCal v4.2 and the Intcal 09 dataset (Bronk Ramsey, 2008; Reimer et al., 2009). These ages are in A.D. notation. The lower age (*) was not included in the age-depth model.

Lab #	Depth (cm)	Measured Age (^{14}C BP)	2σ Calibrated Age Range (A.D.)	Median Calibrated Age	OxCal Modeled Age (A.D.)	Model Agreement	Median Modeled Age
UCI-19881	82.25	630 ± 35	1286-1400	1350	1288-1400	97.6	1353
UCI-19882	117.25	860 ± 35	1046-1260	1180	1053-1257	96.0	1184
UCI-19883	162.25	1100 ± 30	887-1014	940	882-1011	95.3	931
UCI-22766	212.75	1640 ± 40	263-537	410	327-534	96.9	407
UCI-22767	226.25	1770 ± 30	137-345	270	175-386	95.2	297
UCI-14575	228	675 ± 15	646-671*	1290*			

Table DR2. Modern surface water sample stable isotope data and location information.

Sample	Sample Date	Sample Type	Lat (°N)	Lon (°W)	Elev. (m a.s.l.)	$\delta^{18}O$	$\delta^{2}H$
Nejapa	May, 2003	Lake	12.00	86.32	58	3.0	4.9
Moyua	May, 2003	Lake	12.56	86.04	445	-5.4	-39.2
Verde	May, 2003	Lake	11.76	85.96	62	-0.3	-10.6
Blanca	May, 2003	Lake	11.77	85.96	40	-5.6	-39.3
Apoyo Center	May, 2003	Lake	11.94	86.05	73	2.4	8.2
Gancho	June, 2004	Lake	11.91	85.92	42	2.3	-6.0
La Prensa, Ometepe	June, 2004	Spring	11.49	85.55	37	-6.2	-38.9
Maderas	June, 2004	Lake	11.45	85.51	1050	-6.6	-43.3
Charco Verde	June, 2004	Lake	11.48	85.63	70	-0.9	-14.2
Zapatera	June, 2004	Lake	11.77	85.86	42	0.6	-7.8
Apoyo Precip	June, 2004	Rain water	11.94	86.05	200	-1.4	-4.4

Table DR3. Model input and meteorological station data.

Month	Precipitation[a] (mm)	Temperature[b] (ºC)	RH[b] (%)	Extraterrestrial Solar rad. (MJ m^{-2} d^{-1})[b]	Incoming Solar rad. (MJ m^{-2} d^{-1})[c]	$\delta^{18}O_P$ (‰)[d]	δD_P (‰)[d]
Jan	4.1	26.09	73	31.1	16.2	-2.5	-3
Feb	1.1	26.43	72	34.0	19.1	-2.1	-5
Mar	1.1	27.12	70	36.7	20.6	-1.6	-1
Apr	3.0	27.26	73	38.0	17.1	-2.9	-8
May	146.9	26.70	82	38.0	16.0	-1.8	-3
Jun	261.5	26.75	83	37.6	6.0	-1.6	-6
Jul	179.3	26.44	83	37.6	6.8	-3.0	-16
Aug	175.8	26.88	84	37.7	7.9	-2.3	-13
Sep	296.2	26.27	84	36.8	7.0	-5.3	-35
Oct	301.8	26.35	84	34.6	6.6	-5.2	-30
Nov	58.9	26.50	81	31.7	12.0	-6.3	-41
Dec	22.1	26.21	78	30.2	15.1	-5.0	-27

[a] Global Historical Climatology Network (Lawrimore et al., 2011)
[b] MERRA (2004) (1000 hPa pressure level) (Rienecker et al., 2011)
[c] World Survey of Climatology (Portig, 1976)
[d] Bowen and Revenaugh (2003); waterisotopes.org

Table DR4. Model variables and parameters.

RES_L	Surface lake reservoir, m^3	R_a	Extraterrestrial solar radiation, MJ m^{-2} d^{-1}
RES_{CG}	Catchment/groundwater reservoir, m^3	WS	Wind speed, m s^{-1}
F_P	Precipitation on the lake surface, m^3 mon^{-1}	δ_E	Isotopic composition of evaporation, ‰
F_{IN}	Inflow to the lake, m^3 mon^{-1}	δ_L	Isotopic composition of the lake water, ‰
F_E	Evaporation from the lake surface, m^3 mon^{-1}	δ_C	Isotopic composition of calcite, ‰
F_{OUT}	Lake overflow, m^3 mon^{-1}	h_n	Normalized relative humidity, %
F_{CP}	Precipitation input to RES_{CG}, m^3 mon^{-1}	δ_A	Isotopic composition of atm. moisture, ‰
C_{IN}	Catchment inflow delay constant, unitless	ε_{tot}	Total isotopic separation, ‰
C_{CP}	Catchment precipitation constant, m^2	ε_{eq}	Equilibrium isotopic separation, ‰
SA	Lake surface area, m^2	ε_k	Kinetic isotopic separation, ‰
$\alpha_{calcite}$	Equilibrium isotopic fractionation factor, unitless	$e_{s\text{-}a}$	Saturation vapor pressure-air, millibars
T_a / T_w	Air / water temperature, ºC	$e_{s\text{-}w}$	Saturation vapor pressure-water, millibars
P	Precipitation, m mon^{-1}	α	Equilibrium isotopic fractionation factor, unitless
RH	Relative humidity, %	α^*	$1 / \alpha$
R_s	Solar radiation, MJ m^{-2} d^{-1}	C	Kinetic isotopic separation value, ‰

Table DR5. Sensitivity test results (average annual values).

	Model yr	Temp. -2 ºC	Temp. +2 ºC	*RH* -5%	*RH* +5%	Precip. -50%	Precip. +50%	C_{CP}=25	C_{CP}=75	C_{IN}= 0.05	C_{IN}= 0.15
$\delta^{18}O$ (‰ VPDB)	40	-0.37	-0.37	-0.37	-0.37	-0.37	-0.37	0.54	-1.15	-0.41	-0.33
	60	-0.02	-0.72	0.25	-1.04	1.17	-1.46	n/a	n/a	n/a	n/a
$\delta^{18}O$ (‰ VSMOW)	40	1.81	1.81	1.81	1.81	1.81	1.81	2.73	1.03	1.77	1.85
	60	1.77	1.85	2.44	1.15	3.37	0.72	n/a	n/a	n/a	n/a
Res. time (yr)	40	0.32	0.32	0.32	0.32	0.32	0.32	0.40	0.27	0.32	0.32
	60	0.32	0.32	0.32	0.32	0.50	0.24	n/a	n/a	n/a	n/a

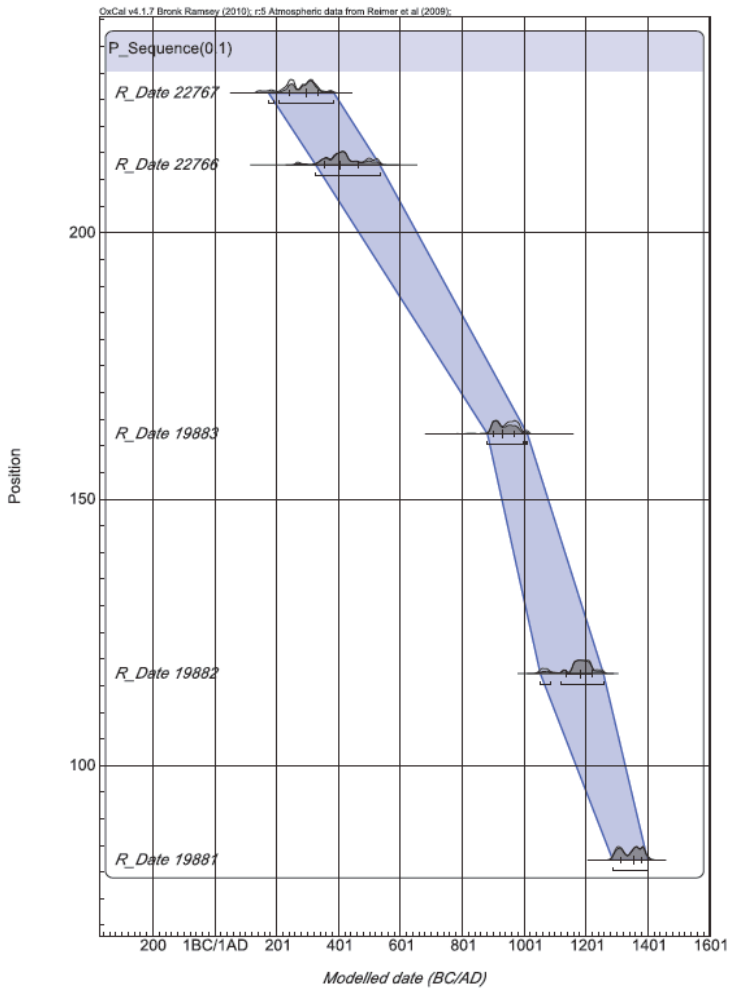

Figure DR1. Detailed age-depth model results with 2-sigma error range from OxCal (Bronk Ramsey, 2008). See Table DR1 for additional information.

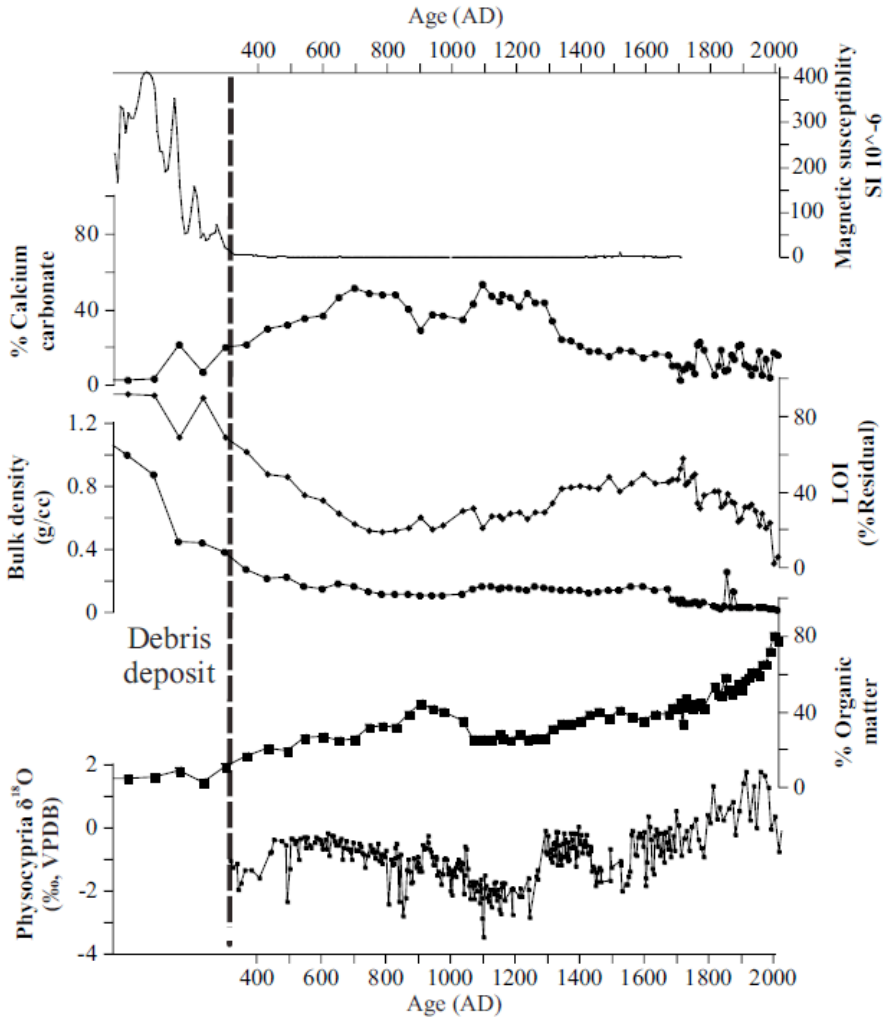

Figure DR2. El Gancho core data plotted versus age. The % Residual LOI data represent the mostly clastic sediment remaining after subtracting the organic matter and calcium-carbonate fractions. The section of the core below ~A.D. 400 is made up of sediment that formed as part of a dry debris avalanche of the Mombacho volcano (Shea et al., 2008). Core data from this section was not included in the main text.

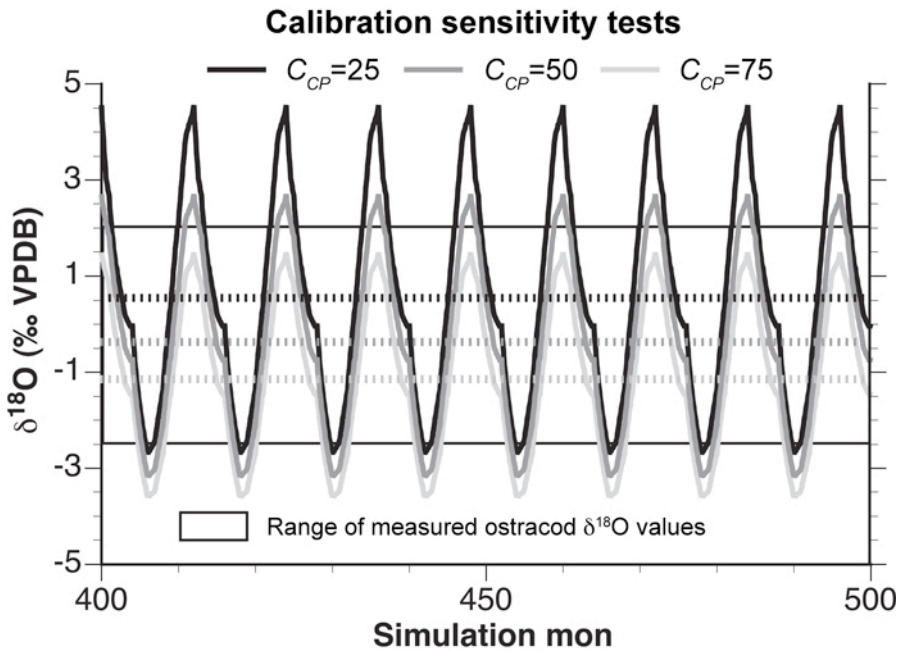

Figure DR3. Simulated El Gancho ostracod $\delta^{18}O$ values from catchment/groundwater parameter sensitivity tests. Solid lines depict continuous monthly values. Dashed lines represent annual average values. The box depicts the range of measured ostracod $\delta^{18}O$ values from the El Gancho sediment core. The C_{CP} parameter was maintained at values of 25 (black line) 50 (dark gray line) and 75 (light gray line) with a value of 50 used in the climate sensitivity simulations.

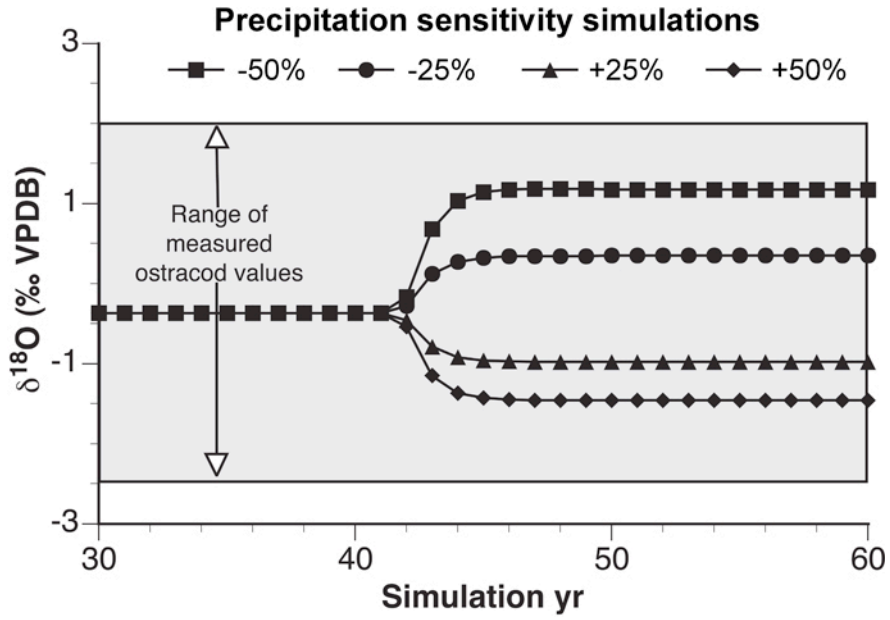

Figure DR4. Ostracod $\delta^{18}O$ values from precipitation sensitivity simulations. Forcing occurs in year 42 and is maintained throughout the simulation. Average annual values are displayed.